# Spectral Filtering Formalism and Its Application for Multi-Phase Deep-Water Wavetrains

*By I. L. Kliakhandler and B. Y. Rubinstein*

A new formalism of spectral filtering for the description of the modulation processes is proposed. The method allows one to study the classical problem of multi-phase modulations in dispersive systems. In the present paper, deep-water waves are considered. Spectral filtering results in a system of coupled equations that describe the modulations of the carrier wave and its harmonics. The formalism may find applications in a broad range of physical situations with multi-phase dynamics.

## 1. Introduction

The present paper is devoted to the well-known problem of multi-phase modulations of wave packets [1], where the wavetrain contains a few carrier interacting frequencies. The introduced general theory of spectral filtering is applied below to the deep-water wave motion.

The classical way to consider the multi-phase wavetrains is through the averaged Lagrangians, though, as was pointed out by Whitham, "... even in ordinary dynamics questions of the existence of quasi-periodic solutions are difficult ones in a nonlinear case, involving the well-known problems of small divisors, so there may be considerable difficulties hidden under the

Address for correspondence: I. L. Kliakhandler, Department of Mathematical Sciences, Michigan Technological University, 1400 Townsend Drive, Houghton, MI 49931-1295, USA; e-mail: igor@mtu.edu

*STUDIES IN APPLIED MATHEMATICS* 110:205–219


Published by Blackwell Publishing, 350 Main Street, Malden, MA 02148, USA, and 9600 Garsington Road, Oxford, OX4 2DQ, UK.

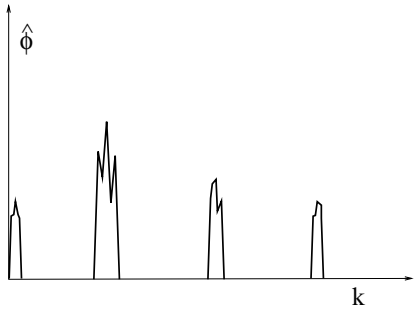


Figure 1. Schematic peaked spectra in multi-phase dynamics.

formalism" (p. 509). Ablowitz and Benney [2] developed the asymptotic theory of multi-phase modulations for the nonlinear Klien–Gordon equation similar to that of Whitham [1]; these ideas were developed further by Ablowitz [3, 4].

In the present study, a new approach to the study of multi-phase dynamics is proposed. Flow parameters are assumed to have peaked spectra, with *finite support* around each peak (Figure 1). It is assumed that during nonlinear dynamics the spectra stay within finite support in Fourier space. Therefore, the modulational dynamics around each peak may be decoupled from each other by the introduction of *spectral filters*. These spectral filters retain the spectral content of the signal near each peak unchanged, and discard everything else (Figure 2). The decoupling results in a system of effectively computable

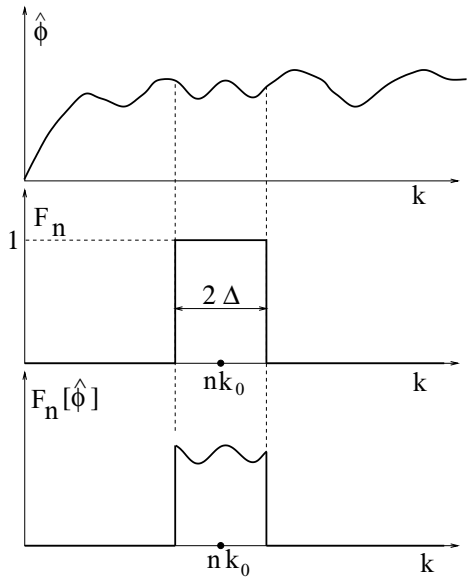


Figure 2. Action of spectral filters.

equations that govern the dynamics of modulations of the carrier wave and its harmonics. The approach is applied to the deep-water wave modulations, where the direct comparison of the stability of the Stokes waves with exact stability computations is possible.

The idea of spectral filters is widely used in radiophysics, electrical engineering, signal processing, speech and pattern recognition, numerical simulations, and many other applied fields. However, as far as we are aware, this is the first application of spectral filters to the derivation of the reduced evolution equation in hydrodynamics.

## 2. New formalism: Peaked spectra and spectral filters

For simplicity, let us consider the case of infinitely deep water; generalization to finite depth is straightforward. We start with the equations for the surface displacement $\zeta(\boldsymbol{x}, t)$ and velocity potential $\phi(\boldsymbol{x}, z, t)$ of an inviscid and incompressible fluid:

$$\frac{\partial \zeta}{\partial t} + \nabla_\perp \phi \cdot \nabla_\perp \zeta = \frac{\partial \phi}{\partial z}, \qquad \frac{\partial \phi}{\partial t} + g\zeta + \frac{1}{2}(\nabla\phi)^2 = 0 \quad \text{at} \quad z = \zeta, \tag{1}$$

$$\nabla^2 \phi = 0 \quad \text{for} \quad -\infty < z < \zeta, \tag{2}$$

$$\frac{\partial \phi}{\partial z} \to 0 \quad \text{at} \quad z \to -\infty. \tag{3}$$

Here $\boldsymbol{x} = (x, y)$ is a horizontal position vector, $z$ is the vertical position, $t$ is time, $\nabla = (\partial/\partial x, \partial/\partial y, \partial/\partial z)$ is the full gradient operator, whereas $\nabla_\perp = (\partial/\partial x, \partial/\partial y)$ is the gradient operator in the horizontal plane; $g$ is the acceleration due to gravity, which without loss of generality is taken to be 1 in the following.

Linear stability analysis of (1)–(3) with respect to the unperturbed system $\bar{\eta} = 0, \bar{\phi} = 0$ gives $\eta = \bar{\eta} + be^{\mathrm{i}(\boldsymbol{k}\cdot\boldsymbol{x}-\omega t)}$, $\phi = \bar{\phi} + ae^{\mathrm{i}(\boldsymbol{k}\cdot\boldsymbol{x}-\omega t)}$, $\omega^2 = |\boldsymbol{k}|$, where $\boldsymbol{k} = (k_x, k_y)$ is the wavenumber, $\omega$ is the frequency. We assume that the flow potential $\phi$ and surface elevation $\zeta$ have *peaked* spectra, like that shown in Figure 1. Its precise meaning is defined below. The full *exact* solution of (2) for potential $\phi$ with a peaked spectrum may be obtained by the Fourier integral

$$\phi = \phi_0 + \tfrac{1}{2}\left(\phi_1 + \phi_1^*\right) + \tfrac{1}{2}\left(\phi_2 + \phi_2^*\right) + \cdots, \tag{4}$$

$$\phi_n = \int_{-\infty}^{\infty} a_n(\boldsymbol{\lambda}, t) e^{\mathrm{i}(n\boldsymbol{k}_0 + \boldsymbol{\lambda})\cdot\boldsymbol{x}} e^{m_n(\boldsymbol{\lambda})z} d\boldsymbol{\lambda},$$

$$m_n(\boldsymbol{\lambda}) = |n\boldsymbol{k}_0 + \boldsymbol{\lambda}| = \omega^2(n\boldsymbol{k}_0 + \boldsymbol{\lambda}). \tag{5}$$

Here $\boldsymbol{k}_0 = (k_{x0}, k_{y0})$ is the carrier wavevector, $\boldsymbol{\lambda} = (\lambda, \mu)$ is the horizontal wave vector. We assume that all $a_n(\boldsymbol{\lambda}, t)$ have *finite support* in Fourier space around 0, i.e., $a_n \equiv 0$ for $|\boldsymbol{\lambda}| > \Delta > 0$. Here $\Delta$ corresponds to half

of the typical spectral width of potential components. As a result, the full spectrum of $\phi$ is assumed to have a number of separated peaks around $n\boldsymbol{k}_0$ for $n = 0, 1, 2, \ldots$, as shown in the stylized Figure 1. The function $m_n(\boldsymbol{\lambda})$ plays an important role in the following, being the essential kernel component in the convolution integrals.

We express the surface displacement $\zeta(\boldsymbol{x}, t)$ as a sum of Fourier integrals:

$$\zeta = \zeta_0 + \frac{1}{2}\left(\zeta_1 + \zeta_1^*\right) + \frac{1}{2}(\zeta_2 + \zeta_2^*) + \cdots, \quad \zeta_n = \int_{-\infty}^{\infty} b_n(\boldsymbol{\lambda}, t) e^{\mathrm{i}(n\boldsymbol{k}_0 + \lambda)\cdot\boldsymbol{x}}\, d\boldsymbol{\lambda}. \tag{6}$$

All $b_n$ are also assumed to have finite support in the Fourier space around 0, i.e., $b_n \equiv 0$ for $|\boldsymbol{\lambda}| > \Delta > 0$. Therefore, the full spectrum of $\zeta$ is also peaked around $n\boldsymbol{k}_0$ for $n = 0, 1, 2, \ldots$.

We make an important assumption, that *during nonlinear interaction all modes $\zeta_n$ and $\phi_n$ preserve finite support in Fourier space*. This assumption is critical for further derivation.

To use spectral filters effectively, a few additional operations are introduced.

1. The value of the potential components on the zeroth level $\Phi_n(\boldsymbol{x}, t) = \phi_n(\boldsymbol{x}, z = 0, t)$. From (4) it follows that

$$\Phi_n(\boldsymbol{x}, t) = \int_{-\infty}^{\infty} a_n(\boldsymbol{\lambda}, t) e^{\mathrm{i}(n\boldsymbol{k}_0 + \boldsymbol{\lambda})\cdot\boldsymbol{x}}\, d\boldsymbol{\lambda}. \tag{7}$$

If $\Phi_n(\boldsymbol{x}, t)$ is known, the corresponding $\phi_n(\boldsymbol{x}, z, t)$ could be easily found,

$$a_n(\boldsymbol{\lambda}, t) = \int_{-\infty}^{\infty} \Phi_n(\boldsymbol{y}, t) e^{-\mathrm{i}(n\boldsymbol{k}_0 + \boldsymbol{\lambda})\cdot\boldsymbol{y}}\, d\boldsymbol{y},$$

$$\phi_n(\boldsymbol{x}, z, t) = \frac{1}{4\pi^2} \int_{-\infty}^{\infty} a_n(\boldsymbol{\lambda}, t) e^{\mathrm{i}(n\boldsymbol{k}_0 + \boldsymbol{\lambda})\cdot\boldsymbol{x}} e^{m_n(\boldsymbol{\lambda})z}\, d\boldsymbol{\lambda}. \tag{8}$$

In the following derivation, the connection between $\Phi_n$ and $\phi_n$ will be exploited.

2. The linear convolution operator $L[\Omega, f]$ which is

$$L[\Omega, f] \equiv \frac{1}{4\pi^2} \int_{-\infty}^{\infty} \int_{-\infty}^{\infty} \Omega(\boldsymbol{\lambda}) e^{\mathrm{i}\boldsymbol{\lambda}\cdot(\boldsymbol{x}-\boldsymbol{y})} f(\boldsymbol{y}, t)\, d\boldsymbol{y}\, d\boldsymbol{\lambda}. \tag{9}$$

In other words, the action of $L[\Omega, f]$ consists of taking the Fourier transform of $f(\boldsymbol{x}, t)$, multiplying the $\boldsymbol{\lambda}$th Fourier coefficient $\hat{f}(\boldsymbol{\lambda})$ on $\Omega(\boldsymbol{\lambda})$, and taking the inverse Fourier transform. In particular, $L[1, f] \equiv f$, and $L[\Omega, Ae^{\mathrm{i}\boldsymbol{k}\boldsymbol{x}}] = A\Omega(\boldsymbol{k})e^{\mathrm{i}\boldsymbol{k}\boldsymbol{x}}$, $A = \text{const}$. If $\Omega(\boldsymbol{\lambda})$ is a polynomial of $(\mathrm{i}\boldsymbol{\lambda})$, the action of $L[\Omega, f]$ may be recast as a usual differentiation operator. As a result, taking the Taylor expansion of $\Omega$ in the power series of $(\mathrm{i}\boldsymbol{\lambda})$, one recovers the "long-wavelength" expansions.

3. The spectral filters $F_n[\Delta, \cdot]$, whose action in Fourier space is

$$F[\Delta, \hat{f}(\boldsymbol{\lambda}, t)] = \begin{cases} 0, & |\boldsymbol{\lambda} - n\boldsymbol{k}_o| \geq \Delta, \\ \hat{f}(\boldsymbol{\lambda}, t), & |\boldsymbol{\lambda} - n\boldsymbol{k}_o| < \Delta. \end{cases} \tag{10}$$

Here $\Delta$ is half of the spectral width of the filter. We assume that $\Delta < |\boldsymbol{k}_0|/2$, so the spectral "windows" of $F_n$ and $F_{n+1}$ do not overlap. The usual Fourier–Galerkin expansions may be considered as spectral filtering with "infinitely narrow" spectral windows. Loosely speaking, the action of filter $F_n$ on the Fourier coefficients $\hat{f}(\boldsymbol{\lambda}, t)$ consists in retaining only the modes around $n\boldsymbol{k}_0$, and discarding the rest of the spectrum (Figures 1 and 2). To illustrate the action of the spectral filters, consider the action of $F_n$ on the full surface elevation $\zeta$,

$$F_n[\Delta, \zeta] = F_n\left[\Delta, \zeta_0 + \tfrac{1}{2}\left(\zeta_1 + \zeta_1^*\right) + \tfrac{1}{2}\left(\zeta_2 + \zeta_2^*\right)\right] = \zeta_n, \tag{11}$$

since all $\zeta_n$ are supposed to have finite support within $2\Delta$ in the Fourier space. It was assumed that the spectra of the flow potential and surface elevation remain in finite spectral support during evolution; hence, the spectral filters may effectively be used to decouple the dynamics around the harmonics $n\boldsymbol{k}_0$.

In the context of deep-water waves, it is convenient to decouple the modulations around the leading carrier wave and its harmonics. In the general case, spectral filters may be applied to various components of the spectra, not necessarily to the harmonics of the leading carrier wave.

4. The procedure of finding $z$-derivatives of the potential components. For example, let us find $\partial\phi_1/\partial z$ on the zeroth level; we will need this and similar quantities in subsequent analysis. From (4) it follows that

$$\left.\frac{\partial \phi_1}{\partial z}\right|_{z=0} = \int_{-\infty}^{\infty} m_1 a_1(\boldsymbol{\lambda}, t) e^{\mathrm{i}(\boldsymbol{k}_0 + \boldsymbol{\lambda})\cdot \boldsymbol{x}}\, d\boldsymbol{\lambda} \equiv L[m_1, \Phi_1]. \tag{12}$$

5. The conventional procedure for the evaluation of the two boundary conditions (1) which are given on the unknown fluid interface $\zeta(\boldsymbol{x}, t)$ through values of all variables at the zeroth level $z = 0$. For the first-order expansion, we have in unfold form

$$\frac{\partial \phi}{\partial t} + g\zeta + \frac{1}{2}\left(\phi_x^2 + \phi_y^2 + \phi_z^2\right) + \phi_{tz}\zeta + (\phi_x\phi_{xz} + \phi_y\phi_{yz} + \phi_z\phi_{zz})\zeta + \frac{1}{2}\phi_{tzz}\zeta^2 = 0 \quad \text{on} \quad z = 0, \tag{13}$$

$$\zeta_t - \phi_z + \zeta_x\phi_x + \zeta_y\phi_y - \phi_{zz}\zeta + \zeta_x\phi_{xz}\zeta + \zeta_y\phi_{yz}\zeta - \tfrac{1}{2}\phi_{zzz}\zeta^2 = 0 \quad \text{on} \quad z = 0. \tag{14}$$

The whole technique works as follows, using the operations introduced above. The expressions for the flow potential and surface elevation from (4) and (6) are substituted in the boundary conditions on the zeroth level (13) and (14). The $z$-derivatives of the potential components are found like in (12) through the action of the operator $L$. The action of the spectral filters on the boundary conditions (13) and (14) allows one to decouple the modulational dynamics near each peak. The decoupling results in a system of two-dimensional equations that govern the dynamics of the surface modulations of the carrier wave and its harmonics.

Let us consider the simplest case which is prompted by the classical Stokes solution. For the Stokes solution, all $\phi_i$ and $\zeta_i$, except $\phi_0$, are just harmonics, i.e., $\phi$ and $\zeta$ have discrete spectra, and the mean surface elevation $\zeta_0$ is usually set to zero. Let us introduce parameter $\varepsilon$, which will measure the amplitude of the first harmonics for surface elevation. We include the variations of $\phi_0$ and $\zeta_0$ into the model, and use Stokes scalings as

$$\phi_1 \sim \zeta_1 \sim \varepsilon, \quad \phi_0 \sim \varepsilon^2, \quad \zeta_0 \sim \varepsilon^2, \quad \phi_2 \sim \zeta_2 \sim \varepsilon^2. \tag{15}$$

We retain the terms up to third order in $\varepsilon$ in (13) and (14), and apply the spectral filters to (13) and (14) near the zeroth, first, and second mode. The final set of six coupled equations for $\zeta_0, \zeta_1, \zeta_2$ and $\Phi_0, \Phi_1, \Phi_2$ will include the terms of various orders; we do not separate them. The result is

$$\frac{\partial \Phi_0}{\partial t} + \zeta_0 + \frac{1}{4}\nabla\phi_1^* \cdot \nabla\phi_1 + \frac{1}{4}L[m_1, \Phi_1]L\left[m_{-1}, \Phi_1^*\right] + \frac{\zeta_1}{4}L\left[m_{-1}, \frac{\partial \Phi_1^*}{\partial t}\right] - \frac{\zeta_1^*}{4}L\left[m_1, \frac{\partial \Phi_1}{\partial t}\right] = 0, \tag{16}$$

$$\frac{\partial \zeta_0}{\partial t} - L[m_0, \Phi_0] - \frac{\zeta_1}{4}L\left[m_{-1}^2, \Phi_1^*\right] - \frac{\zeta^*}{4}L\left[m_1^2, \Phi_1\right] + \frac{1}{4}\nabla\zeta_1 \cdot \nabla\Phi_1^* + \frac{1}{4}\nabla\zeta_1^* \cdot \nabla\Phi_1 = 0, \tag{17}$$

$$\frac{\partial \Phi_2}{\partial t} + \zeta_2 + \frac{1}{4}\nabla\phi_1 \cdot \nabla\phi_1 + \frac{1}{4}L^2[m_1, \Phi_1] + \frac{\zeta_1}{2}L\left[m_1, \frac{\partial \Phi_1}{\partial t}\right] = 0, \tag{18}$$

$$\frac{\partial \zeta_2}{\partial t} - L[m_2, \Phi_2] - \frac{\zeta_1}{2}L\left[m_1^2, \Phi_1\right] + \frac{1}{2}\nabla\zeta_1 \cdot \nabla\Phi_1 = 0, \tag{19}$$

$$\frac{\partial \zeta_1}{\partial t} - L[m_1, \Phi_1] - \zeta_1 L\left[m_0^2, \Phi_0\right] - \frac{\zeta_2}{2}L\left[m_{-1}^2, \Phi_1^*\right] - \zeta_0 L\left[m_1^2, \Phi_1\right] - \frac{\zeta_1^*}{2}L\left[m_2^2, \Phi_2\right] - \frac{\zeta_1^2}{8}L\left[m_{-1}^3, \Phi_1^*\right] - \frac{\zeta_1^*\zeta_1}{4}L\left[m_1^3, \Phi_1\right] + \nabla\zeta_1 \cdot \nabla\Phi_0$$

$$+\nabla\zeta_0\cdot\nabla\Phi_1+\frac{1}{2}\nabla\zeta_2\cdot\nabla\Phi_1^*+\frac{1}{2}\nabla\zeta_1^*\cdot\nabla\Phi_2+\frac{\zeta_1}{4}\nabla\zeta_1\cdot\nabla L\left[m_{-1},\Phi_1^*\right]$$

$$+\frac{\zeta_1}{4}\nabla\zeta_1^*\cdot\nabla L[m_1,\Phi_1]+\frac{\zeta_1}{4}\nabla\zeta_1^*\cdot\nabla L[m_1,\Phi_1]=0, \tag{20}$$

$$\frac{\partial\Phi_1}{\partial t}+\zeta_1+L[m_0,\Phi_0]L[m_1,\Phi_1]+\frac{1}{2}L[m_2,\Phi_2]L\left[m_{-1},\Phi_1^*\right]$$

$$+\frac{\zeta_1}{4}L[m_1,\Phi_1]L\left[m_{-1}^2,\Phi_1^*\right]+\frac{\zeta_1}{4}L\left[m_{-1},\Phi_1^*\right]L\left[m_1^2,\Phi_1\right]$$

$$+\frac{\zeta_1^*}{4}L[m_1,\Phi_1]L\left[m_1^2,\Phi_1\right]+\nabla\Phi_0\cdot\nabla\Phi_1+\frac{1}{2}\nabla\Phi_1^*\cdot\nabla\Phi_2$$

$$+\frac{\zeta_1}{4}\nabla\Phi_1\cdot L\left[m_{-1},\nabla\Phi_1^*\right]+\frac{\zeta_1}{4}\nabla\Phi_1^*\cdot L[m_1,\nabla\Phi_1]$$

$$+\frac{\zeta_1^*}{4}\nabla\Phi_1\cdot L[m_1,\nabla\Phi_1]+\zeta_1 L\left[m_0,\frac{\partial\Phi_0}{\partial t}\right]+\frac{\zeta_1^*}{2}L\left[m_2,\frac{\partial\Phi_2}{\partial t}\right]$$

$$+\frac{\zeta_2}{2}L\left[m_{-1},\frac{\partial\Phi_1^*}{\partial t}\right]+\zeta_0 L\left[m_1,\frac{\partial\Phi_1}{\partial t}\right]+\frac{\zeta_1^2}{8}L\left[m_{-1}^2,\frac{\partial\Phi_1^*}{\partial t}\right]$$

$$+\frac{\zeta_1\zeta_1^*}{4}L\left[m_1^2,\frac{\partial\Phi_1}{\partial t}\right]=0. \tag{21}$$

The structure of Equations (16)–(21) is quite simple. Let us first consider Equation (16), which is extracted from Equation (14) by the application of spectral filter near the zeroth mode. We see that the sum of the indices of $\zeta_i$ and $\phi_i$ in each product term is exactly 0: the first term is $\frac{\partial\Phi_0}{\partial t}$, the second term is $\zeta_0$, the third term is $\frac{1}{4}\nabla\phi_1^*\cdot\nabla\phi_1$, which gives $-1+1=0$, the fourth term is $\frac{1}{4}L[m_1,\Phi_1]L[m_{-1},\Phi_1^*]$, which gives $1-1=0$ (note that the action of the operator $L$ changes the spectral content of the function, but does not shift it), etc. In each equation, the sum of the indices in each term is a constant. Operator $L$ appears in Equations (16)–(21) as a result of taking $z$-derivatives (see (12)).

Equations (16)–(21) are effectively computable. All operations, including the taking of operator $L$, may be effectively performed by fast Fourier transform in a time proportional to $N\log N$, where $N$ is a number of gridpoints. In contrast to that, the computations of the Fourier convolutions in the integral Zakharov equation require computational time proportional to $N^2$ (for quartet interactions), and to $N^3$ for quintet interactions.

## 3. Stokes waves

To obtain a solution of (16)–(21) in the form of classical Stokes waves, consider the case when $\zeta$ and $\phi$ have discrete spectra. We take axis $x$ as being

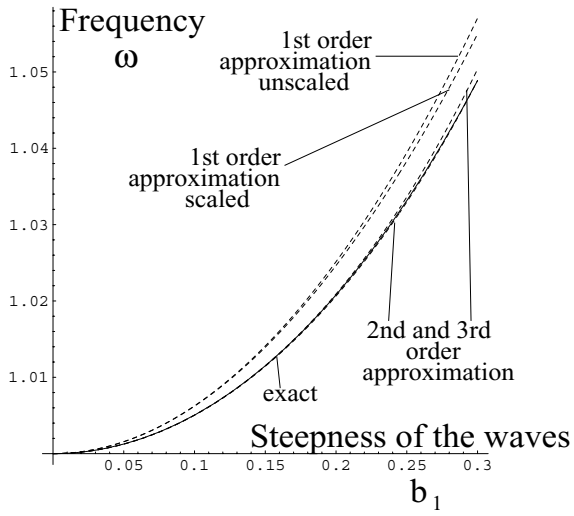


Figure 3. Comparison of discrete-modes solution of various approximations with exact (up to fourth order) Stokes solution.

along the waves, and normalize all wavevectors on the wavenumber of the leading first mode of the Stokes solution; mean elevation is assumed to be zeroth. This results in

$$\zeta_0^S = 0, \quad \zeta_1^S = b_1 e^{\mathrm{i}(x-\omega t)}, \quad \zeta_2^S = b_2 e^{2\mathrm{i}(x-\omega t)}, \quad \Phi_0^S = a_0 t,$$
$$\Phi_1^S = a_1 e^{\mathrm{i}(x-\omega t)}, \quad \Phi_2^S = a_2 e^{2\mathrm{i}(x-\omega t)}. \tag{22}$$

Substitution of (22) in (16)–(21) gives a set of algebraic equations for $\omega$ as a function of the amplitude of the first harmonics of the surface elevation $b_1$. The results of the numerical solution of the equations are shown in Figure 3 as the "first-order approximation scaled." The origin of the other curves will be explained later.

Up to the fourth order in $b_1$, the exact Stokes solution reads [5]

$$\omega = \left[1 + b_1^2 + \tfrac{5}{4} b_1^4\right]^{\frac{1}{2}}. \tag{23}$$

As may be seen from Figure 3, the difference between the discrete-spectrum solution of (16)–(21) and the Stokes solution is of fourth order in the steepness of the waves. The latter is consistent with the corresponding first-order expansion of (1), leading to (16)–(21).

## 4. Stability of Stokes waves, scalings, and expansions

The benchmark test of the validity for the new approach is the stability of the Stokes waves. The linear stability of the two-dimensional NLS equation shows

that the NLS model has a leakage of energy to high-wavenumber modes, with *uniform* maximal growth rate in whole, stretched to infinity, instability domains [6]. Many papers are devoted to the improvement of the NLS equation, beginning with the work by Dysthe [7]; see also the paper by Trulsen and Dysthe [8] with many references. These approaches substantially diminished the energy leakage to the high-wavenumber modes, but did not eliminate it completely.

Typically, the generalization of the NLS equation for a wider bandwidth is done by multiple-scales asymptotic expansions, adding an ever-increasing number of linear dispersive and nonlinear terms in the style of a power series expansion. This approach eventually becomes unattractive due to the lengthy expressions and the poor convergence properties outside some spectral "radius of convergence." Trulsen et al. [9] introduced a new approach based on the exact representation of the linear dispersive term. This method successfully eliminated the energy leakage, and captured well the *quartet* instability regions compared to the exact computations by McLean [10].

The remarkable exact computation of the stability of the Stokes waves by McLean [10] revealed the complex structure of the instability regions. One of the most important conclusions is that in addition to the conventional four-waves (quartet) resonances lying near "figure 8" of Phillips [11], there are five-waves (quintet) resonances which become important for steeper waves. Quintet interactions are not, however, captured by the NLS-based and Trulsen et al. [9] approaches.

The linear stability of the Stokes waves (22) is investigated assuming their small perturbations:

$$(\Phi_0, \zeta_0) = (A_0, B_0)e^{\mathrm{i}(\lambda x+\mu y-\Omega t)} + \text{c.c.}, \tag{24}$$

$$(\Phi_1, \Phi_2, \zeta_1, \zeta_2) = \left(\Phi_1^S, \Phi_2^S, \zeta_1^S, \zeta_2^S\right)\left[1 + (A_1, A_2, B_1, B_2)e^{\mathrm{i}(\lambda x+\mu y-\Omega t)}\right] + \text{c.c.} \tag{25}$$

Here $(\lambda, \mu)$ are the components of the modulational wavevector; $\lambda$ is parallel to the carrier Stokes components, and $\mu$ lies in the orthogonal direction to the carrier components.

The instabilities identified by McLean [10] lie (at least, for small steepnesses) near the curves given by the linear stability analysis of the small-amplitude waves. If the amplitudes of the disturbance harmonics are numbered in an ascending order, the instability curves may be divided into two classes as

Class I

$$[(\lambda + m)^2 + \mu^2]^{\frac{1}{4}} + [(\lambda - m)^2 + \mu^2]^{\frac{1}{4}} = 2m, \tag{26}$$

Class II

$$[(\lambda + m)^2 + \mu^2]^{\frac{1}{4}} + [(\lambda - m - 1)^2 + \mu^2]^{\frac{1}{4}} = 2m + 1. \tag{27}$$

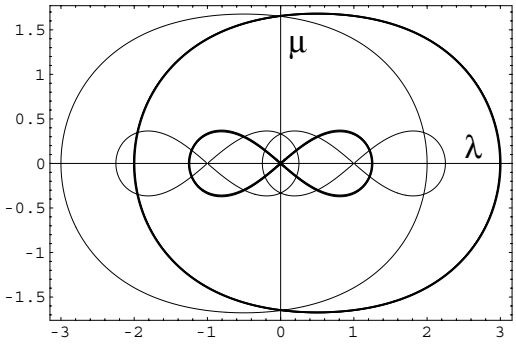


Figure 4. Resonance curves of class I and class II for $m = 1$ from (26) and (27). Conventionally, only one of the curves is shown, which is denoted by a thick line. For the lowest quartet interactions (four-waves resonance), this is the "figure 8." For quintet interactions (five-waves resonance), this is the large, right-shifted curve. All four-waves resonance curves may be obtained as a shift of the thick-line curve in the horizontal direction on an integer; the same is true for five-waves resonance curves.

Here $m$ is an integer. The resonance curve for the first class for $m = 1$ gives the well-known "figure 8" of Phillips [11]. The resonance curve of class II describes quintet interactions. As was already mentioned by McLean [10], there is a degeneracy in his choice of perturbation wavevectors; the shift of the perturbation wavevectors on a whole number of the Stokes carrier wavevectors would just shift the stability diagram. As a result, McLean [10] has shown only the instability diagrams lying near one branch of the resonance curves given by (26) and (27). Taking into account *all* possible resonances, we conclude that the whole set of instability curves lies near the curves given by (26) and (27), *and* their shifts (Figure 4). This consideration gives an indication of the structure of the stability diagram considered below.

Substitution of (24) and (25) into (16)–(21) results in an eigenvalue problem for $\Omega$ as a function of $\lambda$ and $\mu$, which was solved numerically. This eigenvalue problem was very extensively studied in a broad range of $\lambda$ and $\mu$, and for various steepnesses of the Stokes waves. The key element of the numerical procedure is that a large domain in the $(\lambda, \mu)$ plane was "brushed" in search of the instability domains. We have chosen a small increment step equal to 0.001 for $\lambda$ and $\mu$ independently, and have checked *each* point in the $(\lambda, \mu)$ domain using such a small increment in values $\lambda$ and $\mu$. This was done to capture all possible instability domains, and to compare the results of such stability analysis with computations by McLean [10].

The results of the solution of the eigenvalue problem for steepness 0.1 are shown on Figure 5. It should be noted that McLean [10] employed steepness 0.1 based on half the crest-to-trough height of the wave, while the results for Equations (16)–(21) are for steepness 0.1 based on the first harmonic

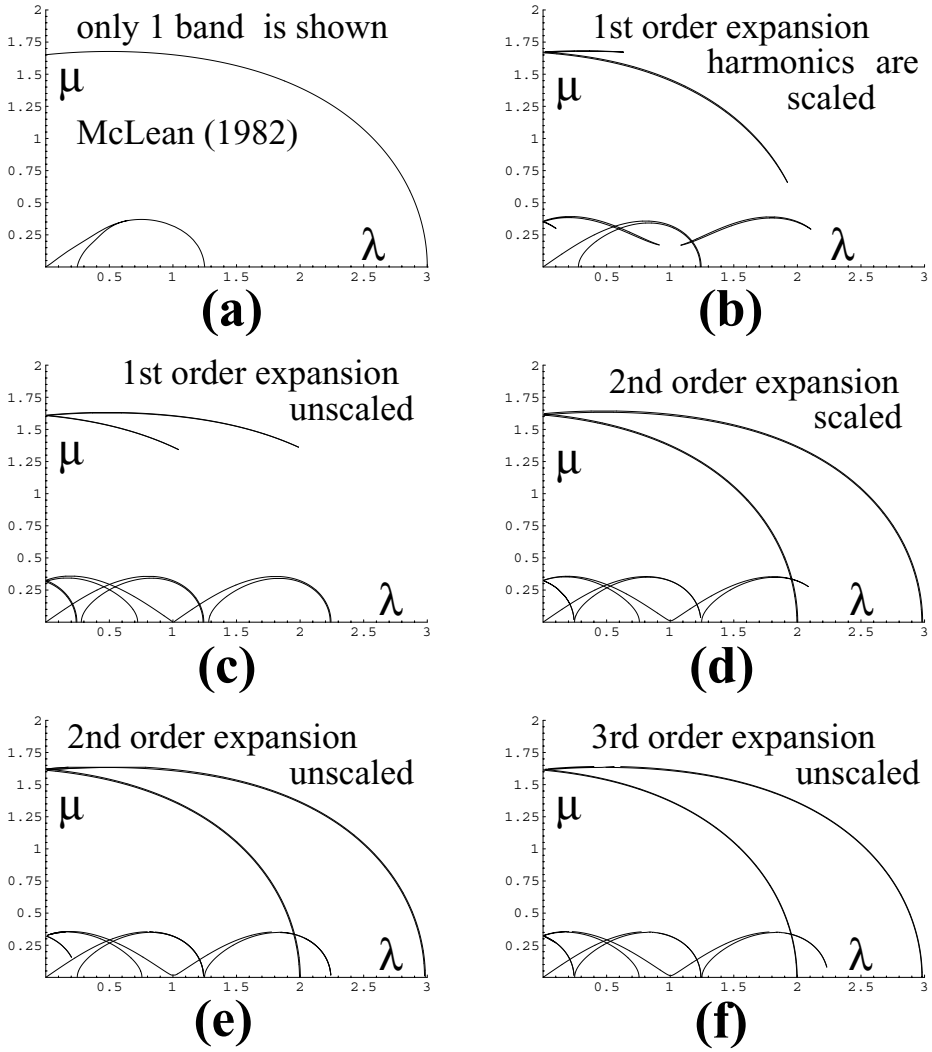


Figure 5. Comparison of the stability analysis based on spectral-filter equations, with exact computation by McLean [9]. Here the steepness is equal to 0.1, and $(\lambda, \mu)$ are the components of the modulational wavevector; $\lambda$ is parallel to the carrier Stokes components, $\mu$ is in orthogonal direction to the carrier components.

amplitude. The difference between these two steepnesses is very small in the present case and can be neglected.

First, compare the results of the McLean instability diagram (Figure 5(a)), the instability diagram for Equations (16)–(21) (Figure 5(b)), and the diagram of all possible resonances in Figure 4. As was mentioned previously, results by McLean [10] show ony one branch of resonances, close to the solid lines in

Figure 4. It is seen that Equations (16)–(21) capture quite well both quartet and quintet resonances given by McLean, and show vestiges of additional resonances similar to those in Figure 4. Since the quintet instabilities are very weak and the domain of the quintet resonances is very thin far from $\lambda = 0.5$ [10], it was impossible to identify them numerically; as a result, the lines of the quintet resonances do not reach the horizontal axis.

As may be seen from a comparison of Figures 4 and 5(b), Equations (16)–(21) somewhat misrepresent the resonances additional to those of McLean. To capture them better, scalings (15) were omitted, and Equations (13) and (14) were filtered without any *a priori* assumptions about the order of all terms. Such an approach results in many new terms additional to those in Equations (16)–(21), which are not presented here. For instance, additional terms will include products such as $(\frac{\partial \phi_0}{\partial x})^2$, $\frac{\partial \phi_2}{\partial y}\frac{\partial \phi_0}{\partial y}$, etc. Results of the stability analysis of those extended equations are shown in Figure 5(c). It is remarkable that all the features of McLean's [10] diagrams are very well reproduced, together with capturing all the resonances, compared with Figure 4. Hence, even a simple first-order unscaled expansion allows one to model multi-resonance modulations. To compare various approximations, many additional simulations were undertaken. Note that Equations (13) and (14) were obtained from (1) using a first-order expansion. In additional simulations, Equations (1) were expanded to second and third orders, with and without scaling (15). Some of the results are shown in Figures 3 and 5(d)–(f). Both expansions improve slightly the first-order approximation, but they include many terms and are probably not practical.

In order to clarify the origin of the various instability regions, additional numerical study of the filtered equations was accomplished. The zeroth component of surface elevation $\zeta_0$ and flow potential $\phi_0$ were set to zero in all equations, and the remaining equations for $\phi_1, \phi_2, \zeta_1, \zeta_2$ were investigated. The results of the equations obtained from first-order expansion of boundary conditions without scalings are shown in Figure 6. It is very interesting that the canonic McLean [10] instability diagram is very well reproduced without additional instability regions.

It is interesting that the already first-order unscaled filtered equations capture the delicate features of McLean diagrams even for bandwidths bigger than 0.5, i.e., in the case where, formally speaking, the initial assumption of isolated spectral contents near different carrier harmonics is violated. Nevertheless, the extensive investigation of the stability of the Stokes waves does not reveal any singularity for $\lambda \geq 0.5$, and reproduces results of McLean [10] very well in the whole range of wavenumbers where the instability has been found, up to values of $\lambda = 3$. All the above leads one to believe that the proposed spectral filtering approach may be used for deciphering multi-phase dynamics in dispersive systems.

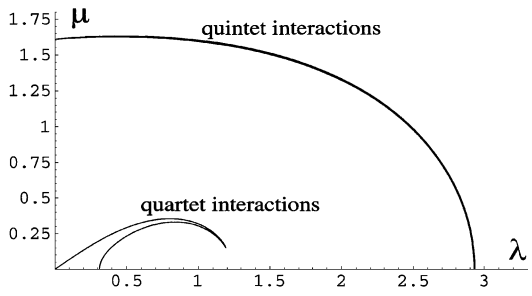


Figure 6. Stability diagram of Stokes waves for truncated filtered equations of the first-order expansion of boundary conditions without scalings of the harmonics.

As a result, the method unifies and extends a few well-known expansion methods: (i) description in terms of discrete modes, where the spectrum is assumed to be a sum of a few delta-functions; (ii) approach of single-mode modulation, where the spectrum is narrow and concentrated near the carrier frequency, and (iii) one-dimensional three-wave interaction technique in optics, where the spectrum is assumed to be narrow-banded near a few carrier frequencies [12]. In the context of the water waves, the equations given by the method may be considered as an alternative to the well-known integral Zakharov equation.

For steep waves, the instability diagram of Stokes waves undergoes a few consecutive changes. First, the instability region detaches from the origin; i.e., very long two-dimensional disturbances parallel to sufficiently steep Stokes waves are stable. For steeper waves, the instability region detaches from the $\lambda$-axis; i.e., any pure two-dimensional disturbances parallel to the Stokes waves are stable. This means that only three-dimensional disturbances may destabilize very steep Stokes waves. Preliminary computations show that Equations (16)–(21) do *not* reproduce these qualitative changes of the stability diagram appearing for very steep Stokes waves (for steepnesses larger than 0.3, not shown here). It looks as if a three-modes representation of the whole wavy spectra is too restricting for such a case. It would be interesting to investigate how to capture the qualitative change of the stability diagram found by McLean [10] for steep waves in the framework of the spectral filtering approach. It is necessary to mention, however, that real ocean waves usually have a very moderate steepness (of order 0.1), so Equations (16)–(21) are expected to work well for the real sea-waves problems.

It is very instructive to consider the difference in the derivation of the Zakharov integral equation with spectrally filtered equations. To make the comparison, we will use a more straightforward derivation of the Zakharov integral equation given by Yuen and Lake [6] than the original derivation by

Zakharov [13]. The key difference is that the ZI equation uses exact boundary conditions instead of their evaluation on the zeroth level as in (13) and (14). The solution of the Laplace equation for the flow potential may be obtained by the Fourier integral, where the Fourier integral contains the term $e^{|\boldsymbol{k}|z}$ (as in (5); see [6], p. 112. To evaluate the term at a moving free surface $z = \zeta(\boldsymbol{x}, t)$, Zakharov expanded the term in the power series of $|\boldsymbol{k}|\zeta$. The expansion appears *in* the Fourier integral, and results in double and triple convolution integrals in the ZI equation. In contrast to that, spectral filtering takes into account the Fourier integrals for the solution of the Laplace equation in their exact form, whereas the boundary conditions at the unknown free surface are approximated by their expansion near the zeroth level. The latter allows one to avoid the appearance of double and triple convolution integrals as in the ZI equation and to obtain computable equations; at the same time, it produces equations with many terms as in Equations (16)–(21). The higher order expansion for the boundary conditions is used, the more terms spectral filtering produces; the number of terms grows rapidly with an increase in the order of expansion.

Note that the outlined procedure allows one to tailor (i) the order of expansion for boundary conditions (1) (third order in (13) and (14)), (ii) the order of various terms as in (15) and their retention, and (iii) the bandwidth of the modes by attribution of some power of $\varepsilon$ to $m_i$ in the operator $L$. This might allow one to ascertain the effectiveness of various asymptotic techniques. Specifically, it provides an opportunity to understand how nonlinearity and bandwidth resolution should be tailored to give the best results and what is the impact of higher order nonlinearities. It would also be very interesting to accomplish full numerical simulations of the derived filtered equations.

## 5. Conclusion

A new spectral filtering approach for deep-water waves is presented. Spectral filters are widely used in many applied fields, such as electrical engineering, speech and pattern recognition, etc. However, as far as we are aware, this is the first application of spectral filters to the derivation of the reduced evolution equation in hydrodynamics.

The proposed spectral filtering allows one to decouple modulations near different carrier harmonics by retention of the spectral content of the waves near those harmonics, and discarding everything else. As a result of the filtering, new equations describing modulations of the carrier harmonics are derived. The essential component of the new equations is that they are effectively computable. The stability analysis of the new equations shows that they reproduce stability diagrams of McLean [10] very well, even for the simplest first-order expansion of the boundary conditions. It is expected that spectral filtering will find applications in a broad range of hydrodynamical situations, both conservative and dissipative.

## References


1. G. B. WHITHAM, *Linear and Nonlinear Waves*, John Wiley & Sons, 1974.
2. M. J. ABLOWITZ and D. J. BENNEY, The evolution of multi-phase modes for nonlinear dispersive waves, *Stud. Appl. Math.* 49:225–238 (1970).
3. M. J. ABLOWITZ, Applications of slowly varying nonlinear dispersive wave theories, *Stud. Appl. Math.* 50:329–344 (1971).
4. M. J. ABLOWITZ, Approximate methods for obtaining multi-phase modes in nonlinear dispersive wave problems, *Stud. Appl. Math.* 51:17–55 (1972).
5. C.-S. YIH, *Fluid Mechanics*, West River Press, 1977.
6. H. C. YUEN and B. M. LAKE, Nonlinear dynamics of deep-water gravity waves, *Adv. Appl. Mech.* 22:67–229 (1982).
7. K. B. DYSTHE, Note on a modification to the nonlinear Schrödinger equation for application to deep water waves, *Proc. R. Soc. Lond. A* 369:105–114 (1979).
8. K. TRULSEN and K. B. DYSTHE, A modified nonlinear Schrödinger equation for broader bandwidth gravity waves on deep water, *Wave Motion* 24:281–289 (1996).
9. K. TRULSEN, I. KLIAKHANDLER, K. B. DYSTHE, and M. G. VELARDE, On weakly nonlinear modulation of waves on deep water, *Phys. Fluids* 12:2432–2437 (2000).
10. J. W. MCLEAN, Instabilities of finite-amplitude water waves, *J. Fluid Mech.* 114:315–330 (1982).
11. O. M. PHILLIPS, On the dynamics of unsteady gravity waves of finite amplitude. Part 1. The elementary interactions, *J. Fluid Mech.* 9:193–217 (1960).
12. D. J. KAUP, A. RIEMAN, and A. BERS, Space-time evolution of nonlinear three-wave interactions. I. interaction in a homogeneous medium, *Rev. Mod. Phys.* 51:275–310 (1979).
13. V. E. ZAKHAROV, Stability of periodic waves of finite amplitude on the surface of a deep fluid, *Jour. Appl. Math. & Tech. Phys.* 9:190–194 (1968).


MICHIGAN TECHNOLOGICAL UNIVERSITY
UNIVERSITY OF CALIFORNIA

(Received April 10, 2002)